

A Kinematic Wave Traffic Flow Model for Mixed Traffic

H. M. Zhang¹

Department of Civil and Environmental Engineering

University of California

Davis, CA 95616

Tel: 530-754-9203

Fax: 530-752-7872

E-mail: hmzhang@ucdavis.edu

W. L. Jin

Department of Mathematics,

University of California

Davis, CA 95616

E-mail: wjin@ucdavis.edu

ABSTRACT

In this paper we extend the Lighthill-Whitham-Richards kinematic wave traffic flow model to describe traffic with different types of vehicles, where all types of vehicles are completely mixed and travel at the same group velocity. A study of such a model with two vehicle classes (e.g., passenger cars and trucks) shows that, when both classes of traffic have identical free-flow speeds, the model 1) satisfies first-in-first-out rule, 2) is anisotropic, and 3) has the usual shock and expansion waves, and a family of contact waves. Different compositions of vehicle classes in this model propagate along contact waves. Such models can be used to study traffic evolution on long crowded highways where low performance vehicles entrap high performance ones.

1 BACKGROUND

Vehicular traffic on highways often comprises different types of vehicles with varying driving performances. This heterogeneity affects traffic flow characteristics in significant ways, a fact that has long been recognized by the transportation engineering profession. For example, in the computation of flow capacity on a highway or at a signalized intersection, the Highway Capacity Manual recommends a series of adjustments to take account of the capacity reduction caused by heavy vehicles (i.e., trucks/buses/recreational vehicles). If one is interested in the effects of heavy vehicles on traffic flow over space and time, however, the Highway Capacity Manual procedures are not adequate. For this one needs a dynamic model for mixed traffic.

Mixed traffic can be modeled at three different levels—microscopic, mesoscopic and macroscopic. It is perhaps most straightforward to model mixed traffic on a microscopic level—one simply endow, at one extreme, each individual vehicle with different performance and behavior characteristics. Many commercially available simulation packages, such as CORSIM, PARAMICS, and VISSIM allow the specification of multiple vehicle classes. Major challenges arise when one models mixed traffic on a mesoscopic level, mainly due to the correlation between various probability distributions of vehicular speeds. Nevertheless, a number of mesoscopic models of mixed traffic have been developed in recent years (1, 2). Aggregation of mesoscopic models of mixed traffic through expectation operations lead to multi-class traffic flow models in the macroscopic level. There is, however, another approach to develop macroscopic mixed traffic flow models. This is the approach of continuum modeling. It is this approach that we shall adopt in developing a traffic flow model for mixed traffic.

In the continuum description of traffic flow, vehicular traffic is described as a special kind of fluid that are characterized by its concentration (density, \mathbf{r}), mean velocity (v), and vehicle flux (flow rate q), all are functions of space (x) and time (t). The starting point of any continuum model of traffic flow is the conservation of vehicles

$$\frac{\partial}{\partial t} \int_{x_1}^{x_2} \mathbf{r}(x, t) dx = q(x_1, t) - q(x_2, t), \quad (1)$$

and the relation between flow, density, and mean velocity $q = kv$.

Equation 1 is an integral form of traffic conservation. When the road segment $[x_1, x_2]$ shrinks to a point in space, one obtains the familiar differential form of traffic conservation:

$$\mathbf{r}_t + q_x = 0, \text{ or } \mathbf{r}_t + (\mathbf{r}v)_x = 0. \quad (2)$$

¹ Author for correspondence.

If one introduces a relation between vehicle concentration and traffic speed $v = V(\mathbf{r})$, one obtains the classic kinematic wave model developed by Lighthill, Whitham (3) and Richards (4):

$$\mathbf{r}_t + (\mathbf{r}V(\mathbf{r}))_x = 0, \quad \mathbf{r}V(\mathbf{r}) \equiv Q(\rho). \quad (3)$$

The classic kinematic wave model of Lighthill and Whitham was formulated for homogeneous flows on a long crowded road. It does not consider the effects of performance differences among different types of vehicles. Recently, Daganzo extended the theory to treat a freeway system with two types of lanes, special lanes and regular lanes, and two types of vehicles, priority vehicles and regular vehicles (5, 6, 7). Priority vehicles are allowed to travel on either regular lanes or special lanes, whereas regular vehicles can only travel on the regular lane. The two types of vehicles in Daganzo's special lane model have different vehicle performances in free-flow traffic, but are indistinguishable in heavy traffic, where both types of vehicles travel at the same speed.

In this paper, we extend the kinematic wave model to vehicular traffic with a mixture of vehicle types. In the mixed flow each vehicle type is conserved and travels at the group velocity, but the differences among vehicle types are accounted for in determining the states of the collective flow. This model can be used to study traffic evolution on long crowded highways where low performance vehicles entrap high performance ones. It can also give a more accurate description of the I-pipe state in Daganzo's special lane model.

The remaining parts of the paper are organized as follows. In Section 2 we give the extended KW model and its basic properties. In Section 3 we analyze the Riemann problem for this model. In Section 4 we propose a fundamental diagram of mixed traffic and discuss its properties. In Section 5 we provide numerical examples and in Section 6 we conclude the paper.

2 THE EXTENDED KW MODEL FOR MIXED TRAFFIC

Let us assume that there are $i = 1, \dots, n$ types of vehicles in the traffic stream ($n \geq 2$), each type has concentration $\rho_i(x; t)$ and velocity $v_i(x; t)$. By conservation of each vehicle type, we have

$$(\mathbf{r}_i)_t + (\mathbf{r}_i v_i)_x = 0, \quad i = 1, \dots, n; \quad (4)$$

As in the development of the classic KW model, we postulate that equilibrium relations exist between vehicular speeds and traffic densities:

$$v_i = V_i(\mathbf{r}_i, \mathbf{r}_n), \quad (5)$$

with $v_i(0) = v_{fi}$, the free-flow speed of each vehicle type and $\partial_{\mathbf{r}_j} V_i < 0$; $i = 1, \dots, n$; $j = 1, \dots, n$.

Equations 4 and 5 are the general governing equations of mixed traffic flow without special lanes. Note that if one adopts $v_i = V(\sum_{i=1}^n \mathbf{r}_i)$, one recovers the I-pipe state in Daganzo's special lane model. In this paper we study a special case of the general equations for mixed traffic in which we consider two types of vehicles—one represents passenger cars (\mathbf{r}_1) and the other represents heavy vehicles such as trucks (\mathbf{r}_2), and two traffic flow regimes—free-flow and congested traffic.

When traffic is light and there are adequate opportunities for passing, different classes of vehicles would travel at their own free-flow speeds v_{fi} . The traffic flow in this case can be described by

$$(\mathbf{r}_i)_t + v_{fi}(\mathbf{r}_i)_x = 0, \quad i = 1, 2. \quad (6)$$

By defining $\mathbf{r} = \sum_{i=1}^n \mathbf{r}_i$, and $v_f = \frac{\sum_{i=1}^n \mathbf{r}_i v_{fi}}{\sum_{i=1}^n \mathbf{r}_i}$, we can use

$$\mathbf{r}_t + (\mathbf{r}v_f)_x = 0 \quad (7)$$

to approximately model the average behavior of light traffic.

When traffic concentration reaches a critical value \mathbf{r}_c , passing opportunities diminish and vehicles of lower performance (e.g. trucks) start to entrap vehicles of higher performance (e.g., passenger cars). Under such conditions it is assumed that the various classes of vehicles are completely mixed and move at the group velocity V . That is, mixed traffic flow in this regime is described by

$$(\mathbf{r}_i)_t + (\mathbf{r}_i V)_x = 0, \quad i = 1, 2. \quad (8)$$

Through the definition of a proper average free-flow speed and the selection of a suitable critical density, we combine Equation 6 (for free-flow traffic) and Equation 8 (for congested traffic) into one modeling equation:

$$\begin{pmatrix} \mathbf{r}_1 \\ \mathbf{r}_2 \end{pmatrix}_t + \begin{pmatrix} \mathbf{r}_1 V(\mathbf{r}_1, \mathbf{r}_2) \\ \mathbf{r}_2 V(\mathbf{r}_1, \mathbf{r}_2) \end{pmatrix}_x = 0, \quad (9)$$

where

$$V(\mathbf{r}_1, \mathbf{r}_2) = \begin{cases} \frac{\sum_{i=1}^n \mathbf{r}_i v_{fi}}{\sum_{i=1}^n \mathbf{r}_i}, & \mathbf{g}_1 \mathbf{r}_1 + \mathbf{g}_2 \mathbf{r}_2 < 1 \\ V_*(\mathbf{r}_1, \mathbf{r}_2), & \mathbf{g}_1 \mathbf{r}_1 + \mathbf{g}_2 \mathbf{r}_2 \geq 1 \end{cases}.$$

Here \mathbf{g}_1 and \mathbf{g}_2 are parameters that determine the critical density in $(\mathbf{r}_1, \mathbf{r}_2)$ coordinates. V_* is a two-dimensional speed-density relation for congested traffic. It is understood that $\partial_{r_i} V_* < 0, i = 1, 2$.

Equation 9 is a system of conservation laws with characteristic velocities:

$$\mathbf{l}_1 = V + \mathbf{r}_1 V_{\mathbf{r}_1} + \mathbf{r}_2 V_{\mathbf{r}_2}, \quad \mathbf{l}_2 = V(\mathbf{r}_1, \mathbf{r}_2).$$

Here we used a special notation for partial derivatives of V with respect to \mathbf{r}_1 and \mathbf{r}_2 : $\partial_{r_1} V \equiv V_{\mathbf{r}_1}$ and $\partial_{r_2} V \equiv V_{\mathbf{r}_2}$.

Owing to the nature of $V(\mathbf{r}_1, \mathbf{r}_2)$, we have $\mathbf{l}_1 \mathbf{l}_2 = V$, that is, both characteristics travel no faster than *average traffic*. In fact, the second characteristic travels at precisely the speed of traffic. When the free-flow speeds of both types of vehicles are identical, the extended KW model preserves the anisotropic property of the KW model. Otherwise, the extended model is not anisotropic in light traffic (the nature of this violation of anisotropy is explained in detail in (8)). Moreover, it can be shown that

$$\left(\frac{\mathbf{r}_2}{\mathbf{r}_1} \right)_t + V \left(\frac{\mathbf{r}_2}{\mathbf{r}_1} \right)_x = 0,$$

from which one obtains $\frac{d}{dt} \left(\frac{\mathbf{r}_2}{\mathbf{r}_1} \right) = 0$, that is, the level curves of $\left(\frac{\mathbf{r}_2}{\mathbf{r}_1} \right)$ in the $t - x$ plane coincide with vehicle

trajectories. The separation of $\left(\frac{\mathbf{r}_2}{\mathbf{r}_1} \right)$ level curves therefore implies first-in-first-out traffic flow behavior between vehicle classes.

Furthermore, the corresponding eigenvectors of the flow Jacobian matrix are

$$\mathbf{r}_1 = \begin{pmatrix} \mathbf{r}_1 \\ \mathbf{r}_2 \\ 1 \end{pmatrix}, \quad \mathbf{r}_2 = \begin{pmatrix} -\frac{V_{\mathbf{r}_2}}{V_{\mathbf{r}_1}} \\ 1 \end{pmatrix}$$

and the Riemann invariants (w, z) , defined as $\nabla w \bullet \mathbf{r}_1 = 0, \nabla z \bullet \mathbf{r}_2 = 0$, are

$$w = \frac{\mathbf{r}_2}{\mathbf{r}_1}, \quad z = V.$$

They are used here to obtain the expansion wave solutions of a Riemann problem (see next section. For more details on Riemann problems and Riemann invariants, refer to (9)).

It can be shown that the first characteristic field is nonlinear and the second characteristic field is linearly degenerate. We therefore have both shock and smooth expansion waves in the first field and contact waves (or slips) in the second field. We shall derive the expressions for these waves related to Riemann data in the next section.

3 RIEMANN PROBLEM AND BASIC WAVE SOLUTIONS

In this section we discuss the solutions of the extended KW model given by Equation 9 with the following so-called Riemann data:

$$\mathbf{r}(x, 0) = \begin{cases} \mathbf{r}^l, & x < 0 \\ \mathbf{r}^r, & x > 0 \end{cases} \quad \mathbf{r} = \begin{pmatrix} \mathbf{r}_1 \\ \mathbf{r}_2 \end{pmatrix}. \quad (10)$$

To solve the above Riemann invariants, we first study the right (downstream) states that can be connected to the left (upstream) states by an elementary wave, i.e., a smooth expansion (rarefaction) wave, a contact, or a shock (readers are referred to (10) and (11, 12, 13, 14) for a more detailed discussion of Riemann problems related to systems of conservation laws in general and traffic flow in particular). Throughout the remaining sections, we assume that $v_{f1} = v_{f2} = v_f$. This assumption ensures that our proposed $V(\mathbf{r}_1, \mathbf{r}_2)$ function is continuous over the entire

feasible $(\mathbf{r}_1, \mathbf{r}_2)$ region. The Riemann problem of Equation 9 with discontinuous $V(\mathbf{r}_1, \mathbf{r}_2)$ is more involved and will be discussed elsewhere. Nevertheless, the analysis of the model given by Equation 9 with $v_{f1} = v_{f2} = v_f$ still reveals many key features of mixed traffic flow.

The 1-expansion waves: An upstream state \mathbf{r}^l can be connected to a downstream state \mathbf{r}^r by a 1-expansion wave if and only if the downstream state satisfies

$$w(\mathbf{r}^l) = w(\mathbf{r}^r), \quad \mathbf{r}^l > \mathbf{r}^r,$$

i.e.,

$$\frac{\mathbf{r}_2^l}{\mathbf{r}_1^l} = \frac{\mathbf{r}_2^r}{\mathbf{r}_1^r}. \quad (11)$$

This means that in the \mathbf{r} -plane the two states are on a ray from the origin. Clearly across an expansion wave traffic composition does not change, that is, vehicles observe the first-in-first-out rule.

The contact waves: A contact wave is a slip that separates two traffic regions of different traffic densities and vehicle compositions but the same travel speed. That is,

$$V(\mathbf{r}^l) = V(\mathbf{r}^r). \quad (12)$$

In the \mathbf{r} -plane, all states on a level curve of $V(\mathbf{r})$ are connected by a contact wave.

The shock waves: The shock waves in the extended KW model are given by the jump condition:

$$s(\mathbf{r}_1^l - \mathbf{r}_1^r) = \mathbf{r}_1^l V(\mathbf{r}_1^l, \mathbf{r}_2^l) - \mathbf{r}_1^r V(\mathbf{r}_1^r, \mathbf{r}_2^r), \quad (13)$$

$$s(\mathbf{r}_2^l - \mathbf{r}_2^r) = \mathbf{r}_2^l V(\mathbf{r}_1^l, \mathbf{r}_2^l) - \mathbf{r}_2^r V(\mathbf{r}_1^r, \mathbf{r}_2^r). \quad (14)$$

After elimination of s from the equations and some algebraic manipulations one obtains

$$(\mathbf{r}_1^l \mathbf{r}_2^r - \mathbf{r}_1^r \mathbf{r}_2^l)(V(\mathbf{r}_1^l, \mathbf{r}_2^l) - V(\mathbf{r}_1^r, \mathbf{r}_2^r)) = 0.$$

Two possibilities exist: $V(\mathbf{r}_1^l, \mathbf{r}_2^l) - V(\mathbf{r}_1^r, \mathbf{r}_2^r) = 0$ which gives the contact waves that we have already discussed, or

$$\mathbf{r}_1^l \mathbf{r}_2^r - \mathbf{r}_1^r \mathbf{r}_2^l = 0, \quad (15)$$

this gives the downstream states \mathbf{r}^r that can be connected to the upstream state \mathbf{r}^l by a shock. Note that all these states also fall on a ray originating from the origin of the \mathbf{r} -plane. This implies that across a shock vehicle composition also does not change, that is, vehicles observe first-in-first-out rule. Moreover, we have the following entropy conditions

$$\mathbf{r}^l < \mathbf{r}^r$$

to ensure the stability of the shock.

Now we can state the procedure to solve a Riemann problem for the extended KW model. Note that for any state \mathbf{r}^l , the two curves/lines given by Equations 11 and 12 divide the feasible \mathbf{r} -plane into four regions (Figure 1). If the downstream state \mathbf{r}^r falls on any of these two curves/lines, it can be connected to the upstream state by an elementary wave. If it falls on any of the four regions, however, an intermediate state \mathbf{r}^m is generated on the line given by Equation 11, which is connected with the upstream state by a 1-wave (i.e., an expansion or shock wave) and with the downstream state by a contact (Figure 1). Figure 2 shows a few examples of Riemann solutions.

4 FUNDAMENTAL DIAGRAMS FOR MIXED TRAFFIC

We propose the following $\mathbf{r}-V$ relation, which can be derived from a car-following model under steady-state conditions (15), to be used in the mixed traffic flow model.

$$V = \begin{cases} \frac{\mathbf{r}_1 v_{f1} + \mathbf{r}_2 v_{f2}}{\mathbf{r}_1 + \mathbf{r}_2}, & (l_1 + \mathbf{t}_1 v_{f1})\mathbf{r}_1 + (l_2 + \mathbf{t}_2 v_{f2})\mathbf{r}_2 < 1 \\ \frac{1 - \mathbf{r}_1 l_1 - \mathbf{r}_2 l_2}{\mathbf{r}_1 \mathbf{t}_1 + \mathbf{r}_2 \mathbf{t}_2}, & (l_1 + \mathbf{t}_1 v_{f1})\mathbf{r}_1 + (l_2 + \mathbf{t}_2 v_{f2})\mathbf{r}_2 \geq 1 \end{cases}$$

We call the above relation the extended speed-density relation for the triangular fundamental diagram. The parameters are: free flow speeds for both types of vehicles v_{f1} and v_{f2} , effective vehicle lengths for type-1 and type-2 vehicles l_1 and l_2 , and response times of type-1 and type-2 vehicles t_1 and t_2 . The last two parameters capture, to a certain degree, the acceleration/deceleration differences between the two classes of vehicles.

The capacity of mixed flow depends on vehicle composition. For example, in the case of $v_{f1} = v_{f2} = v_f$,

let $\frac{r_2}{r_1} = p < \infty$, then the critical densities of the proposed speed-density relation are

$$r_{1c} = \frac{1}{(l_1 + pl_2) + v_f(t_1 + pt_2)}, \quad r_{2c} = pr_{1c}.$$

Note that when $p = 0$, i.e., there are no type-2 vehicles in the traffic stream, we recover the critical density for type-1 vehicles

$$r_{1c} = \frac{1}{l_1 + v_f t_1}$$

and when $p = \infty$, i.e., no type-1 vehicles present in the traffic stream, we can switch the positions of p in relation to l 's and t 's in the above formulas and replace it with $\frac{1}{p} = 0$. Again we recover the critical density for type-2 vehicles

$$r_{2c} = \frac{1}{l_2 + v_f t_2}$$

For any vehicle mixture (i.e. $0 < p < \infty$), the capacity flow is $\left(\frac{v_f}{l_2 + v_f t_2}, \frac{v_f}{l_1 + v_f t_1} \right)$.

5 NUMERICAL SOLUTION METHOD AND SIMULATIONS

5.1 The Godunov Method

We approximate the mixed traffic KW model with the Godunov method (16):

$$\begin{aligned} \frac{r_{1,i}^{j+1} - r_{1,i}^j}{\Delta t} + \frac{r_{1,i+1/2}^{*j} V(r_{1,i+1/2}^{*j}, r_{2,i+1/2}^{*j}) - r_{1,i-1/2}^{*j} V(r_{1,i-1/2}^{*j}, r_{2,i-1/2}^{*j})}{\Delta x} &= 0, \\ \frac{r_{2,i}^{j+1} - r_{2,i}^j}{\Delta t} + \frac{r_{2,i+1/2}^{*j} V(r_{1,i+1/2}^{*j}, r_{2,i+1/2}^{*j}) - r_{2,i-1/2}^{*j} V(r_{1,i-1/2}^{*j}, r_{2,i-1/2}^{*j})}{\Delta x} &= 0, \end{aligned}$$

in which $r_{k,i}^j$ is the average of r_k over cell i at time t_j ; i.e., $r_{k,i}^j = \int_{x=x_{i-1/2}}^{x_{i+1/2}} r_k(x, t_j) dx / \Delta x$, and $r_{k,i-1/2}^{*j}$ is the average over time interval $[t_j, t_{j+1}]$ at the boundary $x_{i-1/2}$ between cells i and $i-1$; i.e.,

$r_{k,i-1/2}^{*j} = \frac{1}{\Delta t} \int_{t=t_j}^{t_{j+1}} r_k(x_{i-1/2}, t) dt$. Given (r_1, r_2) at t_j , we hence can compute traffic states at the following time t_{j+1} .

In the above equations, the boundary average $r_{k,i-1/2}^{*j}$ can be found by solving the Riemann problem for the extended KW model, given by Equation 9, with the following initial condition $(r^l = (r_{1,i-1}^j - r_{2,i-1}^j)$ and $r^r = (r_{1,i}^j, r_{2,i}^j))$

$$\mathbf{r} = \begin{cases} \mathbf{r}^l, & \text{if } x - x_{i-1/2} < 0, \\ \mathbf{r}^r, & \text{if } x - x_{i-1/2} > 0. \end{cases}$$

As shown in section 2, the Riemann solutions consist of a shock or rarefaction wave with an intermediate state \mathbf{r}^m and a contact wave. Since all the waves are self-similar, we have $\mathbf{r}_{i-1/2}^{*j} = \mathbf{r}(x_{i-1/2}, t) = \text{const}$ for all $t > 0$, which is determined by the shock or rarefaction wave connecting \mathbf{r}^l and \mathbf{r}^m since the contact wave has non-negative velocity and is not involved.

From Equations 11 and 15, we have

$$\frac{\mathbf{r}_2^l}{\mathbf{r}_1^l} = \frac{\mathbf{r}_2^m}{\mathbf{r}_1^m}, \quad (16)$$

and from Equation 12

$$V(\mathbf{r}^m) = V(\mathbf{r}^r). \quad (17)$$

Combining Equations 16 and 17, we can find the intermediate state \mathbf{r}^m , from which we can compute $\mathbf{r}_{i-1/2}^{*j}$ as described in the following cases.

Case 1. When $\mathbf{r}^l < \mathbf{r}^m$, they are connected by a shock, and the shock speed is

$$s = \frac{\mathbf{r}_1^l V(\mathbf{r}_1^l, \mathbf{r}_2^l) - \mathbf{r}_1^m V(\mathbf{r}_1^m, \mathbf{r}_2^m)}{\mathbf{r}_1^l - \mathbf{r}_1^m} \quad (18)$$

In this case, solutions of $\mathbf{r}_{i-1/2}^{*j}$ are summarized in Table 1.

Case 2. When $\mathbf{r}^l > \mathbf{r}^m$, they are connected by a rarefaction wave, in which the characteristic velocity is $l_1(\mathbf{r}_1, \mathbf{r}_2)$, and $l_1(\mathbf{r}^l) < l_1(\mathbf{r}^m)$. If $l_1(\mathbf{r}^l) \geq 0$, $\mathbf{r}_{i-1/2}^{*j}$ is the same as the left state \mathbf{r}^l ; if $l_1(\mathbf{r}^m) \leq 0$, it is the same as the intermediate state \mathbf{r}^m . Otherwise, $\mathbf{r}_{i-1/2}^{*j}$ satisfies

$$\begin{aligned} l_1(\mathbf{r}_{1,i-1/2}^{*j}, \mathbf{r}_{2,i-1/2}^{*j}) &= 0, \\ \mathbf{r}_{2,i-1/2}^{*j} / \mathbf{r}_{1,i-1/2}^{*j} &= \mathbf{r}_2^l / \mathbf{r}_1^l, \end{aligned} \quad (19)$$

which implies that $\mathbf{r}_{i-1/2}^{*j}$ maximizes the total flow $(\mathbf{r}_1 + \mathbf{r}_2)V(\mathbf{r}_1, \mathbf{r}_2)$ along the line $\mathbf{r}_2 / \mathbf{r}_1 = \mathbf{r}_2^l / \mathbf{r}_1^l$. In this case, therefore, solutions of $\mathbf{r}_{i-1/2}^{*j}$ are summarized in Table 2.

5.2 Numerical Simulations

In our simulations, we will use the extended triangular fundamental diagram (Figure 3), in which the parameter values are: free flow speed for both types of vehicles $v_{f1} = v_{f2} = v_f = 65 \text{ mph} = 95.3333 \text{ ft/sec}$, effective vehicle lengths for type-1 and type-2 vehicles: $l_1 = 20 \text{ ft}$, $l_2 = 40 \text{ ft}$, and response times of type-1 and type-2 vehicles: $t_1 = 1.5 \text{ s}$, $t_2 = 3 \text{ s}$. Therefore, we have $\mathbf{r}_{1,\text{jam}} = 1/l_1 = 0.05 \text{ veh/ft}$ and $\mathbf{r}_{2,\text{jam}} = 1/l_2 = 0.025 \text{ veh/ft}$. Moreover, since $l_1/l_2 = t_1/t_2$, we have that in the extended triangular fundamental diagram $V(\mathbf{r}_1, \mathbf{r}_2)$ is a function of $\mathbf{r}_1 / \mathbf{r}_{1,\text{jam}} + \mathbf{r}_2 / \mathbf{r}_{2,\text{jam}}$. Thus, as we will see later, the evolution pattern of travel speed is the same as that of $\mathbf{r}_1 / \mathbf{r}_{1,\text{jam}} + \mathbf{r}_2 / \mathbf{r}_{2,\text{jam}}$.

We will conduct numerical simulations for a ring road, whose length $L = 2000l_1 = 40,000 \text{ ft}$, during a time interval from $t = 0$ to $T = 100t_1 = 150 \text{ s}$. In order to apply the Godunov method, we partition the ring road into $N = 1000$ cells with length $\Delta x = L/N = 40 \text{ ft}$, and discretize the time interval to $M = N/2$ steps with the duration of each time step $= T/M = 0.3 \text{ s}$. Since the CFL (Courant, Friedrichs, and Lewy) condition number (17)

$$\max\{|I_1|, |I_2|\} \frac{\Delta t}{\Delta x} \leq v_f \frac{\Delta t}{\Delta x} = 0.715 < 1,$$

the Godunov method yields convergent solutions.

For the numerical simulations, we use the following global perturbation as initial traffic conditions,

$$\begin{aligned} \mathbf{r}_1(x, 0) &= (0.2 + 0.16 \sin(2\pi x / L)) \mathbf{r}_{1, \text{jam}}, \\ \mathbf{r}_2(x, 0) &= (0.15 + 0.1 \sin(2\pi x / L)) \mathbf{r}_{2, \text{jam}}, \end{aligned} \quad (20)$$

in which the density of the 1-type vehicles, i.e., has higher average but smaller oscillation.

With these conditions, the solutions of the mixed traffic flow model are depicted as contour plots and shown in Figure 4. The horizontal axis in each of the sub figures represents space and the vertical axis time. These figures depict the traffic conditions (speed and density). As shown in the contour plots of v and $\mathbf{r}_1 / \mathbf{r}_{1, \text{jam}} + \mathbf{r}_2 / \mathbf{r}_{2, \text{jam}}$, there are roughly two traffic regions along the ring road initially. In one region

$(l_1 + t_1 v_f) \mathbf{r}_1 + (l_2 + t_2 v_f) \mathbf{r}_2 \geq 1$, waves initiated from this region travel backward in the same speed, which is

$$l_1(\mathbf{r}_1, \mathbf{r}_2) = -(\mathbf{r}_1 l_1 + \mathbf{r}_2 l_2) / (\mathbf{r}_1 t_1 + \mathbf{r}_2 t_2) = -l_1 / t_1 = -40 / 3 \text{ ft/sec.}$$

In another region, where $(l_1 + t_1 v_f) \mathbf{r}_1 + (l_2 + t_2 v_f) \mathbf{r}_2 < 1$, waves initiated from this region travel forward at free-flow speed. Two waves separate the two regions: an expansion wave on the left and a shock wave on the right. The shock wave travels forward initially but eventually travels at $-l_1 / t_1$ as traffic density increases to critical density in the second (free-flow) region. The patterns of the solutions of \mathbf{r}_1 and \mathbf{r}_2 , however, are not the same as that of v because the change of the overall traffic conditions affect each vehicle class differently.

The contour plot of $\mathbf{r}_2 / \mathbf{r}_1$ is given in Figure 5, from which we can see that the level curves do not intersect. Remembering that the level curves of $\mathbf{r}_2 / \mathbf{r}_1$ coincide with vehicle trajectories, the solutions shown here indicate that under the given conditions first-in-first-out rule is respected by the mixed flow model. From this figure we can also see the expansion and shock waves as they move through traffic, which are marked by changes in the slopes of the level curves.

6 CONCLUDING REMARKS

In this paper we extend the Lighthill-Whitham-Richards kinematic wave traffic flow model to describe traffic with different types of vehicles, where all types of vehicles are completely mixed and travel at the same group velocity. A study of such a model with two vehicle classes (e.g., passenger cars and trucks) shows that, when both classes of traffic have identical free-flow speeds, the model 1) satisfies first-in-first-out rule, 2) is anisotropic, and 3) has the usual shock and expansion waves, and a family of contact waves. Different compositions of vehicle classes in this model propagate along contact waves. Such models can be used to study traffic evolution on long crowded highways where low performance vehicles entrap high performance ones.

REFERENCES

1. Helbing, D. *Verkehrsdynamik. Neue physikalische Modellierungskonzepte*. Springer, Berlin, 1997.
2. Hoogendoorn, S. P. and P. H. L. Bovy. Modeling multiple user-class traffic flow. *Transpn Res. B*, Vol. 34, No. 2, 2000, pp. 123-146.
3. Lighthill, M. J. and G. B. Whitham. On kinematic waves: Ii. a theory of traffic flow on long crowded roads. In *Proc. Royal Society*, 229(1178) of A, 1955, pp. 317-345.
4. Richards, P. I. Shock waves on the highway. *Operations Research*, Vol. 4, 1956, pp. 42-51.
5. Daganzo, C. F. A continuum theory of traffic dynamics for freeways with special lanes. *Transpn Res. B*, Vol. 31, 1997, pp. 83-102.
6. Daganzo, C. F., W. H. Lin, and J. M. Del Castillo. A simple physical principle for the simulation of freeways with special lanes and priority vehicles, *Transpn Res. B*, 1997, pp. 103-105.
7. Daganzo, C. F. A behavioral theory of multi-lane traffic flow Part I: Long homogeneous freeway sections. UCB-ITS-RR-99-5, 1999.
8. Zhang, H. M. Anisotropic property revisited—does it hold in multilane traffic? Working paper, Institute of Transportation Studies, Davis. To appear in *Trans. Res. B*, 2000.
9. Whitham, G. B. *Linear and nonlinear waves*. John Wiley & Sons, New York, 1974.

10. LeVeque, R. *Numerical methods for conservation laws*, Birkhauser Verlag, 1993.
11. Aw, A. and M. Rascle. Resurrection of "Second Order" Models of Traffic Flow. *SIAM Appl. Math.* Vol. 60, No. 3, 2000, pp. 916-938.
12. Zhang, H. M. Structural properties of solutions arising from a nonequilibrium traffic flow theory. *Trans. Res. B*, Vol. 34, 2000, pp. 583-603.
13. Zhang, H. M. A non-equilibrium traffic flow model devoid of gas-like behavior. To appear in *Trans. Res. B*, 2000.
14. Zhang, H. M. New perspectives on continuum traffic flow models. *Special issue on traffic flow theory*, H. M. Zhang, ed., *J. of Networks and Spatial Econ.*, Vol. 1, Issue 1, 2001, pp. 9-33.
15. Zhang, H. M. and T. W. Kim. Transient and steady state behavior of car-following in mixed traffic on a ring road. Working paper, Institute of Transportation Studies, Davis, 2000.
16. Godunov, S.K. Bounds on the discrepancy of approximate solutions constructed for the equations of gas dynamics. *J. Com. Math. And Math. Phys. I*, 1961, pp. 623-637.
17. Courant, R., K. Friedrichs, and H. Lewy. ber die partiellen Differenzengleichungen der mathematischen Physik, *Math. Ann.* 100, 1928, pp. 32-74.

List of tables

Table 1. Shock Solution

Table 2. Rarefaction Wave Solution

List of figures

Figure 1: Phase diagram for determining elementary and simple waves

Figure 2: Wave solutions to the Riemann problem: Shock + Contact wave (left) and Expansion wave + Contact wave (right) (In the bottom figures, thick (dashed) lines are characteristics, and lines with arrows are vehicles' trajectories.)

Figure 3: The extended triangular fundamental diagram

Figure 4: Contour plots of solutions on the $x - t$ space with the extended triangular fundamental diagram

Figure 5: Contour plot of ρ_2/ρ_1 on the $x - t$ space with the extended triangular fundamental diagram

TABLE 1 Shock Solution

s given in Equation 18	$\mathbf{r}_{1,i-1/2}^{*j}$	$\mathbf{r}_{2,i-1/2}^{*j}$
$s > 0$	\mathbf{r}_1^l	\mathbf{r}_2^l
$s \leq 0$	\mathbf{r}_1^m	\mathbf{r}_2^m

TABLE 2 Rarefaction Wave Solution

\boldsymbol{l}_1	$\boldsymbol{r}_{1,i-1/2}^{*j}$	$\boldsymbol{r}_{2,i-1/2}^{*j}$
$\boldsymbol{l}_1(\boldsymbol{r}^l) \geq 0$	\boldsymbol{r}_1^l	\boldsymbol{r}_2^l
$\boldsymbol{l}_2(\boldsymbol{r}^m) \geq 0$	\boldsymbol{r}_1^m	\boldsymbol{r}_2^m
o.w.	given in Equation 19	

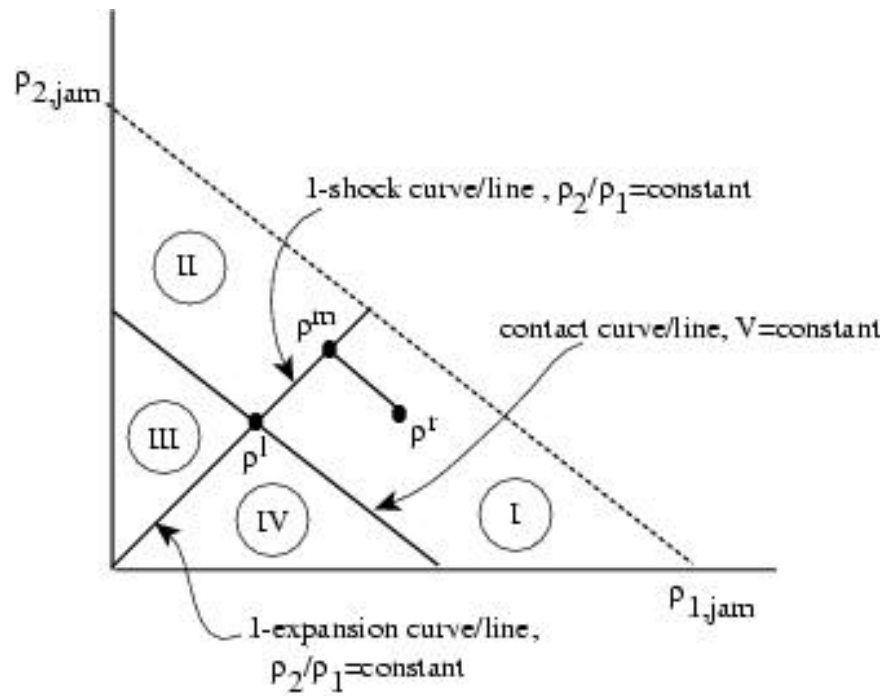


FIGURE 1 Phase diagram for determining elementary and simple waves

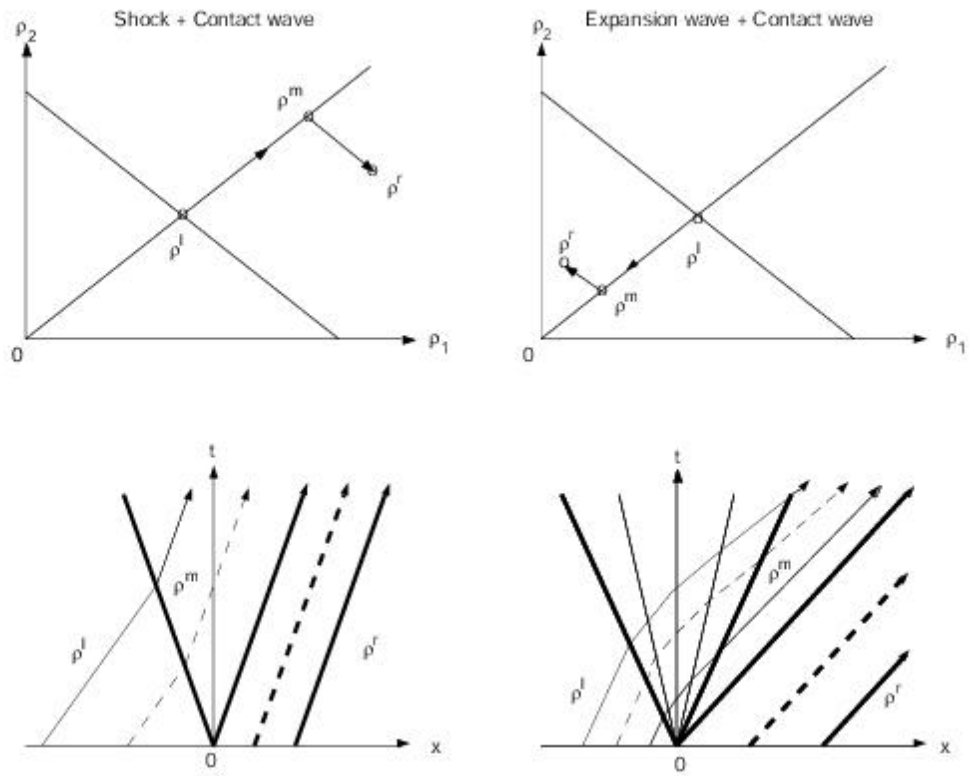


FIGURE 2 Wave solutions to the Riemann problem: Shock + Contact wave (left) and Expansion wave + Contact wave (right) (In the bottom figures, thick (dashed) lines are characteristics, and lines with arrows are vehicles' trajectories.)

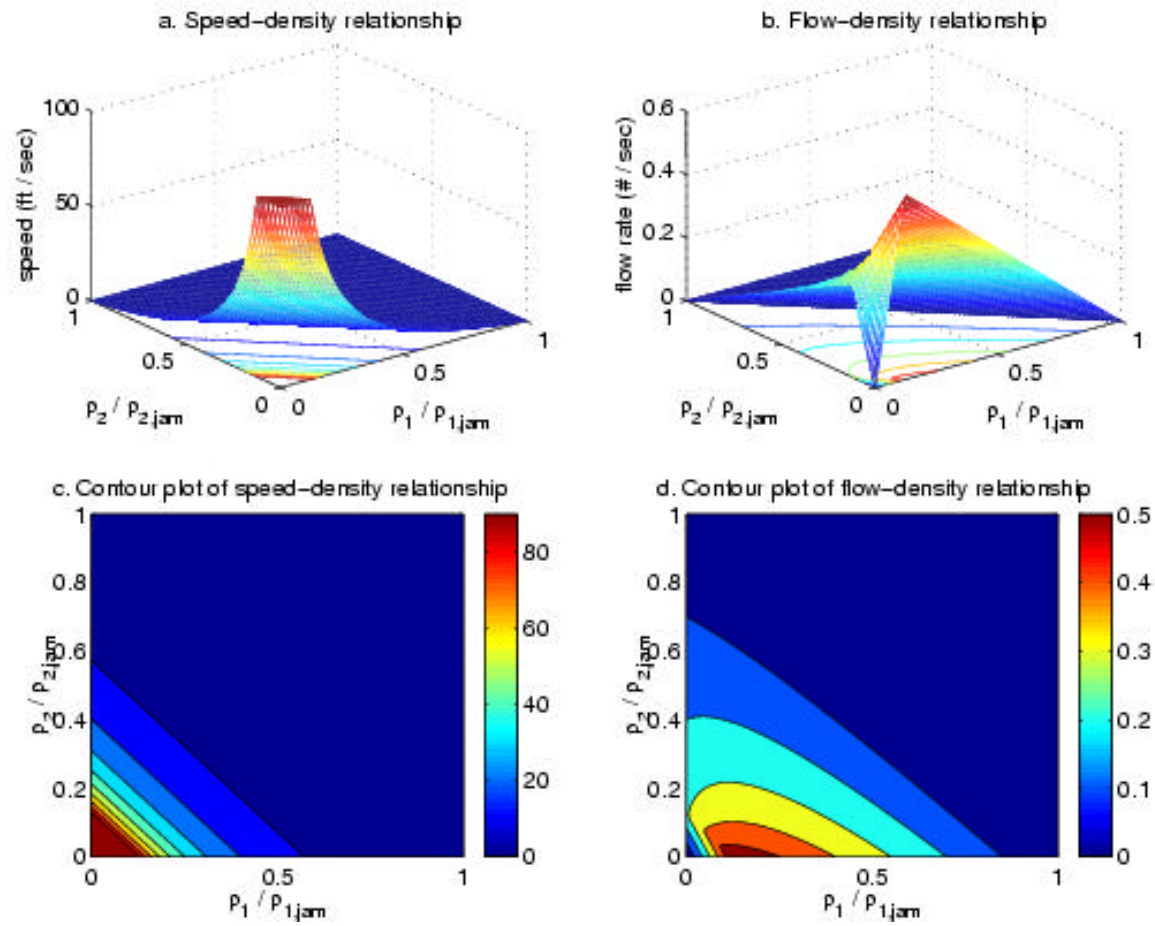


FIGURE 3 The extended triangular fundamental diagram

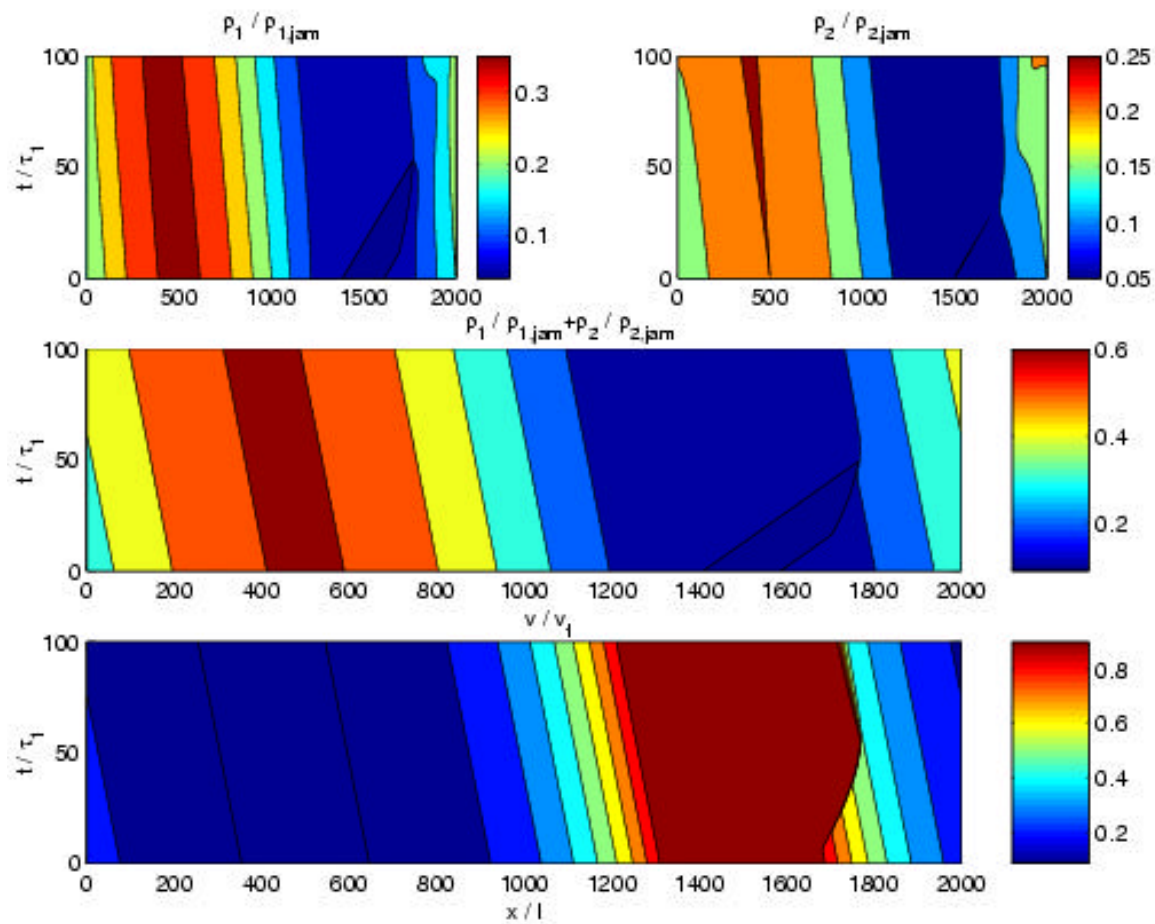


FIGURE 4 Contour plots of solutions on the $x - t$ space with the extended triangular fundamental diagram

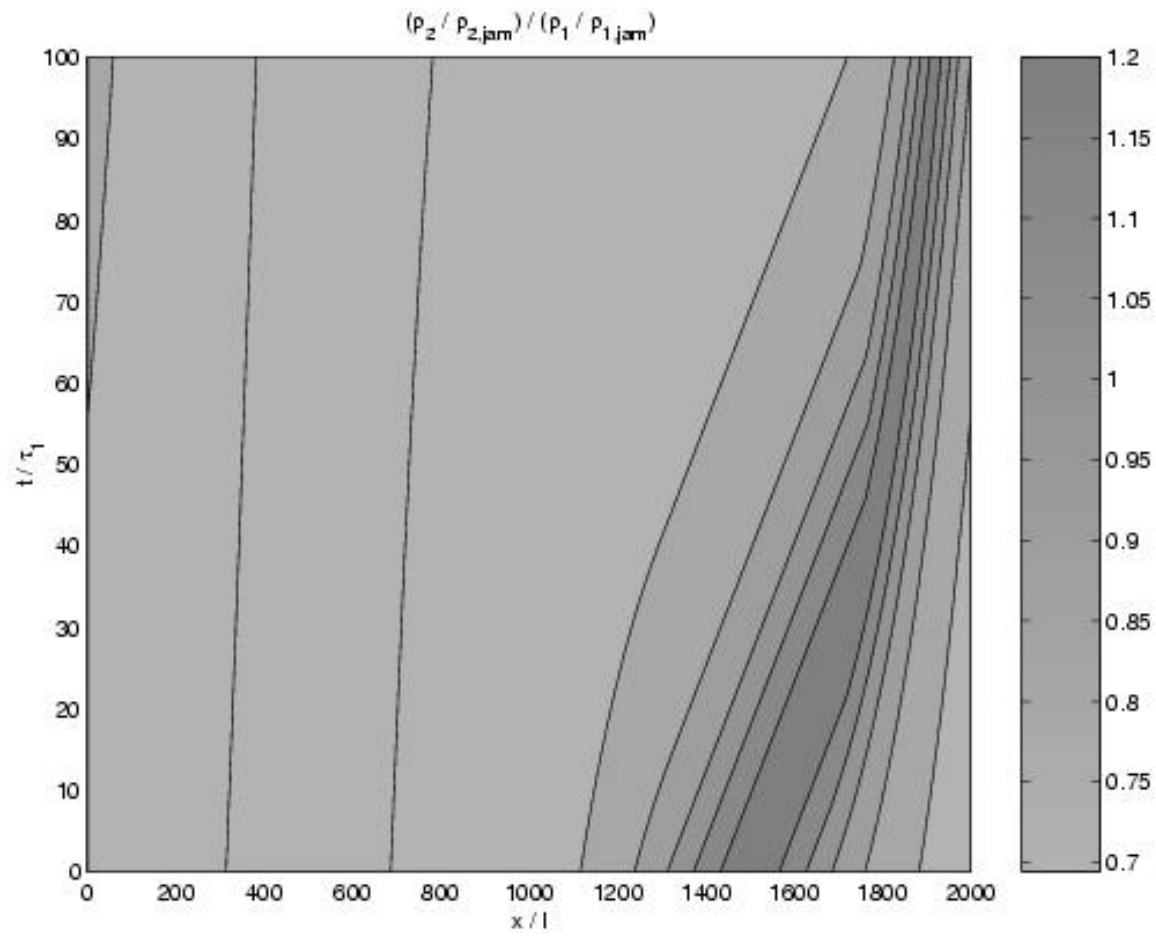


FIGURE 5 Contour plot of ρ_2/ρ_1 on the $x - t$ space with the extended triangular fundamental diagram